

Increased Brain Tumor Resection Using Fluorescence Image Guidance in a Preclinical Model

Arjen Bogaards, BSc,^{1,2} Abhay Varma, MD,² Sean P. Collens, MAsc,¹ Aihua Lin, MD,¹ Anoja Giles, BSc,¹ Victor X.D. Yang, MAsc,¹ Juan M. Bilbao, MD,³ Lothar D. Lilje, PhD,¹ Paul J. Muller, MD,² and Brian C. Wilson, PhD^{1*}

¹Department of Medical Biophysics, Ontario Cancer Institute/University Health Network and University of Toronto, Toronto, Ontario, Canada M5G 2M9

²Division of Neurosurgery, St. Michael's Hospital, Toronto, Ontario, Canada M5B 1W8

³Division of Pathology, St. Michael's Hospital, Toronto, Ontario, Canada M5B 1W8

Background and Objectives: Fluorescence image-guided brain tumor resection is thought to assist neurosurgeons by visualizing those tumor margins that merge imperceptibly into normal brain tissue and, hence, are difficult to identify. We compared resection completeness and residual tumor, determined by histopathology, after white light resection (WLR) using an operating microscope versus additional fluorescence guided resection (FGR).

Study Design/Materials and Methods: We employed an intracranial VX2 tumor in a preclinical rabbit model and a fluorescence imaging/spectroscopy system, exciting and detecting the fluorescence of protoporphyrin IX (PpIX) induced endogenously by administering 5-aminolevulinic acid (ALA) at 4 hours before surgery.

Results: Using FGR in addition to WLR significantly increased resection completeness by a factor 1.4 from 68 ± 38 to $98 \pm 3.5\%$, and decreased the amount of residual tumor post-resection by a factor 16 from 32 ± 38 to $2.0 \pm 3.5\%$ of the initial tumor volume.

Conclusions: Additional FGR increased completeness of resection and enabled more consistent resections between cases. *Lasers Surg. Med.* 35:181–190, 2004.

© 2004 Wiley-Liss, Inc.

Key words: malignant glioma; VX2; 5-aminolevulinic acid; protoporphyrin IX; fluorescence imaging and spectroscopy

INTRODUCTION

The treatment of patients with high-grade gliomas remains a major challenge. The prognosis for these patients is poor, with a median survival time after diagnosis and treatment of less than 1 year [1,2]. It has been suggested that the prognosis is linked to the completeness of tumor removal [3–6]. A recent [7] study of 416 patients with glioblastoma multiforme indicated that resection of 89% of the tumor volume is necessary to improve survival, while resection of 98% or more resulted in a significant survival advantage of 4.2 months compared with a resection of less than 98%. However, such a high degree of tumor resection

is often limited by the surgeon's ability to distinguish residual tumor tissue from surrounding brain tissue under conventional white light microscope illumination [8]. Hence, methods enabling better intraoperative discrimination of viable tumor borders should be valuable.

Fluorescence imaging and spectroscopy using 5-aminolevulinic acid (ALA)-induced protoporphyrin IX (PpIX) is a potential technique to enhance contrast of viable tumor borders. Although administration of fluorescent markers to enhance contrast of malignant gliomas is not new [9–13], marking tumors with ALA is conceptually different from earlier investigations, since ALA is not itself fluorescent but is metabolized into fluorescent PpIX by a number of malignant tumors in situ through enzymes of the heme-biosynthesis pathway [14]. ALA-PpIX has been used widely, both for fluorescence diagnostics and photodynamic therapy [15]. It may avoid problems that arise when a fluorescent marker is administered directly, such as leakage from the tumor into surrounding normal brain tissue [16]. We have shown previously [17–20] that ALA-induced PpIX levels in normal brain tissue, especially white matter, are very low. Clinical and preclinical studies suggest that the resulting selectivity of ALA-PpIX in certain brain tumors [14,17–25] is a result of various factors. The low permeability of ALA at the blood–brain barrier (BBB) [17,26] reduces uptake in normal brain, whereas the compromised BBB in certain brain tumors is thought to permit selective ALA transport. Different activities of enzymes in the heme pathway have also been observed between tumor and normal tissues, which subsequently enable selective production of PpIX [27,28].

Contract grant sponsor: NIH; Contract grant number: CA 43892; Contract grant sponsor: DUSA Pharmaceuticals NY.

*Correspondence to: Dr. Brian C. Wilson, PhD, University Health Network/Ontario Cancer Institute, 610 University Avenue, Room 7-417, Toronto, Ont., Canada M5G 2M9.

E-mail: wilson@uhnres.utoronto.ca

Accepted 17 June 2004

Published online in Wiley InterScience
(www.interscience.wiley.com).

DOI 10.1002/lsm.20088

Stummer et al. recently introduced ALA-PpIX fluorescence imaging for intra-operative detection and resection of residual malignant glioma in 52 patients using an operating microscope adapted for fluorescence imaging [8,23]. ALA was administered orally at a dose of 20 mg/kg at 3 hours before induction of anesthesia and subsequent surgery. They observed that leaving “solidly fluorescing” tissue unresected had a negative influence on survival, whereas the prognosis of patients with residual “vague fluorescence” was not significantly different from that of patients in whom all solid fluorescent tissue was completely removed. Histologically, solidly fluorescing tissue was characterized mostly by coalescent tumor cells, whereas vaguely fluorescing tissue usually represented infiltrating tumor of intermediate or low cellular density. However, analysis of tumor biopsy specimens revealed infiltrating tumor also to be present beyond vaguely fluorescing tissue portions. This is an important study in demonstrating the potential of ALA-PpIX FGR, but is limited by the facts that only a single ALA dose and time interval were used and that the assessment of the tissue fluorescence was qualitative and subjective. We hypothesize that more quantitative fluorescence-based detection will further improve this technique and, therefore, we have developed a system for quantitative fluorescence imaging and image-guided point fluorescence spectroscopy. We have previously described this instrument and its initial demonstration for brain tumor fluorescence imaging in a pilot study in patients undergoing Photofrin-photodynamic therapy [12].

In the present study, we have used this system for FGR in an intracranial tumor-bearing rabbit model, with the primary objective to compare completeness of tumor resection and residual tumor volume after white light resection (WLR) versus additional ALA-PpIX fluorescence-guided resection. These values were quantified by histology of resected tissues and of the whole brain after resection. As a secondary objective, we determined the tumor-to-normal ratio in tissues resected under white light as well as in tissues resected under fluorescence guidance. These experiments were done using a fixed ALA dose and time interval, as a precursor to planned clinical and preclinical glioma resection studies to optimize these two factors.

MATERIALS AND METHODS

Optical Design of Co-Axial Fluorescence Imaging and Spectroscopy System

The fluorescence imaging/spectroscopy system [12] is an optical illumination and detection platform specifically designed for open-field surgical procedures (Fig. 1). Mounted on a suspension arm, this system illuminates the surgical field uniformly across the field of view (FOV) with 405 nm light at 6 mW cm^{-2} , matching the main absorption peak of PpIX. The illumination light is integral to the camera and coaxial with the imaging pathway, i.e., it is a “point and shoot” device. The fluorescence emitted from the tissue is imaged onto a CCD camera with 755×484 pixels at 10-bit dynamic range, that is mounted behind a filter wheel containing five different band pass filters (20 nm FWHM)

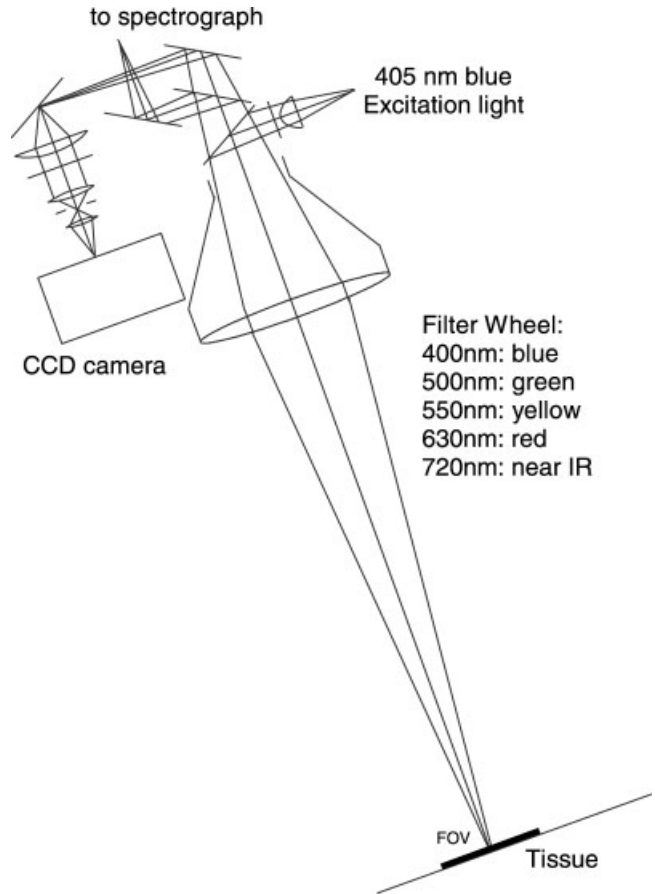


Fig. 1. Optical design of the co-axial multi-spectral fluorescence imaging and spectroscopy system, the bar indicates the field of view (FOV) of the camera: details are found in Ref. [12].

within the spectral range of 480–720 (Omega, Brattleboro, NJ). These have an OD of >7 in the blue/UV range to reject the excitation light. The total acquisition time for five spectral images and a full fluorescence emission spectrum is approximately 30 seconds. To obtain a quantitative fluorescence image various image processing algorithms can be performed on these five spectral images, which also requires approximately 30 seconds. Also, the system is capable of white-light imaging using the normal operating room lighting, by combining the red, green, and blue channels. The working distance is 50 cm, which allows the camera head to be positioned while not impeding surgical access. The FOV is 3.3×2.5 cm and the depth of focus is 2 cm, adequate for the geometry of open-field neurosurgery. The spatial resolution is 0.15 mm. A spectrograph, integrated with the fluorescence imaging system, performs non-contact fluorescence spectroscopy over a small area (diameter ~ 0.6 mm) within the surgical field, at locations selected in the image FOV by the operator. The positioning of the system is similar to that of conventional operating microscopes with manual suspension arms, although more time consuming in the present prototype configuration.

Tumor Propagation and Induction

This study was approved by the Animal Care Committee of St. Michael's Hospital, Toronto (ACC512). We elected to use rabbits in this first animal study, since this allows fairly large tumors (5–10 mm diameter), which simplifies the surgical procedures compared to smaller animal models. Since there is no glioma model in the rabbit, we used the VX2 carcinoma, which has similarities in its growth characteristics to primary brain tumors, such as micro-invasion, pseudo palisading, growth along the blood vessels and in perivascular spaces, and breakdown of the BBB within the tumor and in brain adjacent to tumor [19]. We have reported the use of this model previously for studies of ALA-PpIX distribution and photodynamic therapy response [18–20]. Male SPF New Zealand white rabbits (3.3–3.8 kg) (Charles River, Montreal, QC, Canada) were used to propagate the tumor cell line by injecting a suspension of 10^6 VX2 cells in 1 ml PBS (phosphate buffered saline) at three locations into the left adductor magnus muscle. These animals were euthanized 14–25 days post-induction by i.v. injection of T61 (Intervet, Whitby, Ont., Canada). The tumors were approximately 1 cm diameter when harvested and the VX2 cells were extracted using a strainer. Subsequently, the cells were counted in PBS with a haemocytometer and used within 2 hours. For intracranial induction, the animals were anaesthetized with a mixture of 5 mg/kg Xylazine (Bayer, Germany) and 50 mg/kg Ketamine (de Wyet-Ayerst, Guelph, Ont., Canada) and the site was shaved and swabbed with betadine (Purdue Frederick, Pickering, Ont., Canada). A 2–3 cm midline incision was made, the scalp reflected and the cranium exposed. Using a 1.5 mm diameter drill, a burr hole was performed over the right hemisphere, anterior to the coronal suture and 5 mm to the right of the bregma, leaving the dura intact. A 100 μ l Hamilton syringe was introduced to a depth of 3 mm beneath the dura and 10^5 VX2 cells in 50 μ l PBS were inoculated intracerebrally, over a period of 2–3 minutes with low pressure to avoid trauma. Bone wax was used to close the burr hole and the incision was then closed with sutures. Buprenex (Reckitt&Colman Ltd., Hull, England) was administered subcutaneously for analgesia every 8 hours for the first 24 hours post-implantation. Fourteen animals received VX2 cells and three animals were injected with saline and used as controls.

Resection Procedure

Surgery was performed 14 days post-VX2 induction and 4 hours post i.v. injection of 20 mg/kg ALA in hydrochloride form (Levulan, DUSA Pharmaceuticals, Valhalla, NY) as a solution in PBS buffered to pH 6.2–6.8. For surgery, the animals were brought under general anesthesia by subcutaneous Xylazine/Ketamine injection, with Buprenex used for systemic analgesia. The eyes were lubricated with Lacri-Lube (Allergan, Inc., Markham, Ont., Canada) and closed with tape to prevent exposure to the operating and blue excitation light. The heart rate and oxygen saturation were monitored with a pulse oximeter (Model 8500V; Nonin Medical, Plymouth, MN). The head was fixed in position in

a stereotaxic frame with a rabbit adapter (Model 900; David Kopf Instr., Tujunga, CA). The scalp was shaved, betadine was applied to the surgical site, which was covered with a sterile keyhole drape, and the incision site was injected with 1–2 cc of 2% Xylocaine (Astra Zeneca, Mississauga, Ont., Canada). A 2–4 cm incision was made in the scalp along the mid-line and held open with a self-retaining retractor. A craniotomy was performed using a small hand-held orthopedic drill of 1.5 mm diameter, which was continuously cooled with sterile betadine saline solution. Gentle suction was used to remove irrigating fluid and bone dust. The bone flap was gently elevated with a periosteal elevator, aiming to keep the entire dura intact. Once the bone flap was removed, both left and right hemispheres were exposed and the dura was cut using microsurgery scissors and forceps.

White Light Resection

The tumor was located and removed under white light illumination using an operating microscope. Bipolar coagulation was used as required. Saline irrigation and suction were used to keep the surgical site clean and a micro-pituitary forceps with a 2-mm tip to was used to remove the tumor tissue. Care was taken to minimize removal of normal brain. WLR was considered complete once no tumor tissue was visible to the neurosurgeon using the operating microscope under white light illumination.

Fluorescence Guided Resection

Once WLR was completed, point fluorescence spectra and images were acquired in the surgical cavity (Fig. 2). Since the fluorescence signal is weak, FGR was performed with the operating light switched off and the ambient light was subdued. We aimed to resect (and save) all fluorescing tissues. FGR was considered complete once the fluorescence intensity throughout the surgical cavity had decreased to the background level of the surrounding brain. Since all resected tissues were saved for histology, care was taken to remove tissues only by biopsy forceps and not by suction. Immediately following completion of tumor resection, the animals were euthanized by i.v. T61 injection and the whole brain was removed intact. White light resected tissues, fluorescence guided resected tissues, and whole brain were saved in separate, light-tight containers and immediately snap frozen in liquid nitrogen and stored until further use at -70°C .

Fluorescence Quantification

In the present study, the full quantitative capabilities of the fluorescence imaging system could not be exploited, since the acquisition time and image processing time of approximately 60 seconds allowed the surgical cavity to fill with blood, obstructing the blue excitation and red fluorescence light. Hence, we were forced to obtain fluorescence images in real-time (30 frames per second), by using only the red fluorescence channel (640 nm), combined with suction to clear the surgical site of blood. As a result, we obtained relatively poor anatomical definition. Also,



Fig. 2. Surgical experimental setup showing (1) the fluorescence imaging system, (2) the operating microscope, and (3) the rabbit covered with a sterile keyhole drape.

although the camera gain, integration time, excitation power, and focal distance were held constant, the fluorescence signal was only partially quantitative, since other factors, such as the tissue optical properties, autofluorescence and background light, were not determined.

Histopathology and Volume Calculations

Serial sections of $5\ \mu\text{m}$ thickness were prepared at $0.5\ \text{mm}$ intervals and stained with hematoxylin and eosin (H&E). Slides were digitized using a stereomicroscope (Model MZFLIII; Leica, Germany) with a digital camera (DC300F), using $1\text{--}10\times$ objectives. For consistency, areas of normal and tumor tissue were delineated by a single investigator (SPC) on these low magnification images using Image Pro-Plus software (Media Cybernetics, Silver Spring, MD), while observing the original slide under a microscope (Optiphot; Nikon, Japan) at higher magnifications using $10\text{--}40\times$ objectives. This investigator was trained by a neuro histopathologist (JMB), who verified the delineated

region of tumor and normal tissue on every 7th slide. Both investigators were blinded to the resections. Pixel size calibration allowed calculation of the cross-sectional area of each region, and the separation between sections then enabled the volumes of tumor and normal tissues to be calculated. The percentage of residual tumor (RT) after WLR, RT_w , after fluorescence resection, RT_f , and after white light plus FGR, RT_{w+f} , were defined as,

$$RT_w = \frac{T_f + T_{wb}}{T_w + T_f + T_{wb}} \times 100\%,$$

$$RT_f = \frac{T_w + T_{wb}}{T_w + T_f + T_{wb}} \times 100\%,$$

$$RT_{w+f} = \frac{T_{wb}}{T_w + T_f + T_{wb}} \times 100\%,$$

where T_w , T_f , and T_{wb} are, respectively, the tumor volume in the white light resected tissues, in the fluorescence resected tissues and in the whole brain at the end of the procedure. We note that, using blue excitation light and given the known camera sensitivity, the effective depth for fluorescence detection below the tissue surface is likely less than $0.5\ \text{mm}$ [12]. Hence, in the calculation of T_{wb} we did not include tumor located at a distance more than $0.5\ \text{mm}$ away from the surgical cavity. The percentage of tumor resection completeness in the whole brain after WLR, TRC_w , fluorescence resection, TRC_f , and white light plus fluorescence resection, TRC_{w+f} , were defined here as, $TRC_{\text{sub}} = 100\% - RT_{\text{sub}}$. In order to compare WLR and additional FGR, we performed one-sample *t*-tests on the groups RT_w versus RT_{w+f} and TRC_w versus TRC_{w+f} .

RESULTS

White Light Resection

Under white light, the tumor appeared grayish white that was distinct from surrounding white matter, often with areas of hemorrhage and cystic necrosis. All the abnormal appearing tissue was removed until only normal white matter was observed in the tumor bed. In 11 of 14 animals, the tumor was visible under white light illumination, whereas in three animals the tumor was not visible under white light but a small region of fluorescence was found and resected.

Fluorescence Guided Resection

No fluorescence was detected in the three non-tumor bearing control animals while resecting up to $7\ \text{mm}$ beneath the dura, which was deeper than in the tumor-bearing animals. False positive fluorescence was consistently observed in choroid plexus and optical nerves. PpIX fluorescence was present in all 14 tumor-bearing animals, verified by point spectroscopy that showed the characteristic PpIX peaks at 635 and $704\ \text{nm}$. A typical fluorescence image is illustrated in Figure 3. In two animals, fluorescence resection was not completed, since the tumor invaded deeply into the brain and complete resection would have been fatal.

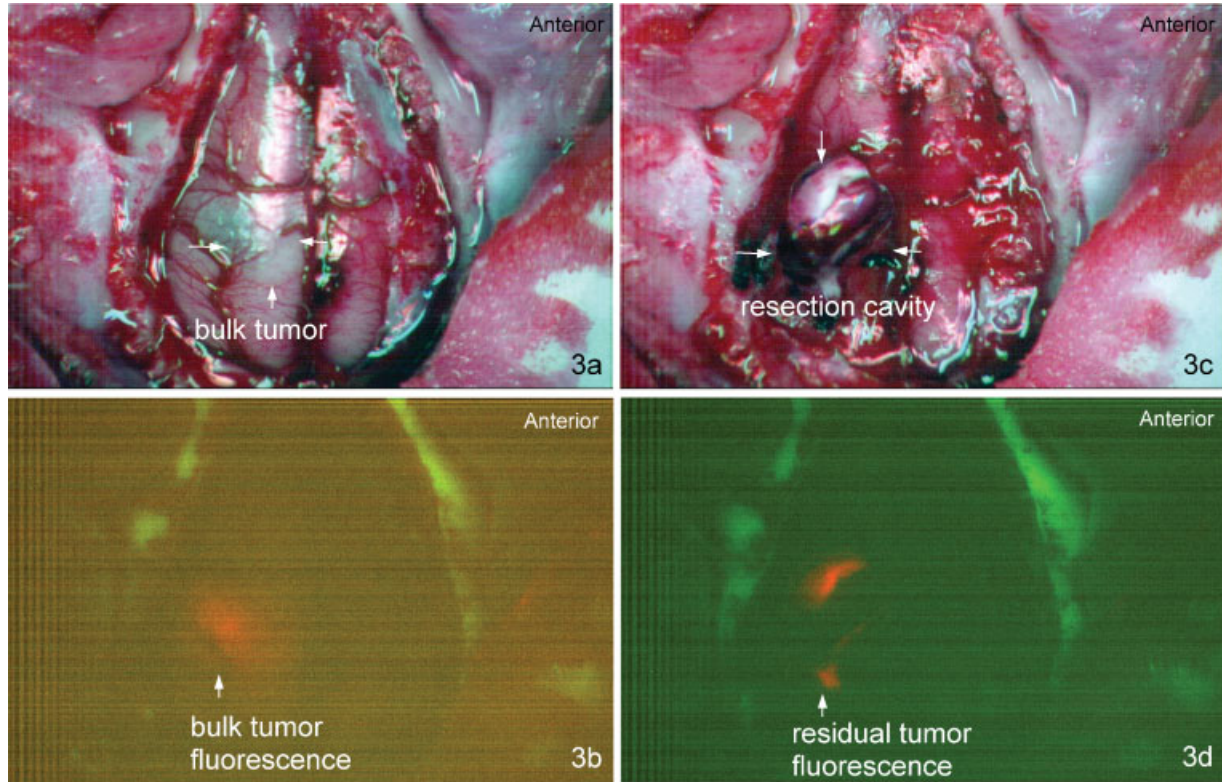


Fig. 3. Example of white light (a, c) and fluorescence (b, d) imaging in VX2 rabbit brain. a: Shows the brain surface before resection, with visible, white-appearing VX2 tumor. b: Shows the corresponding fluorescence image, where the bulk tumor fluoresces in red. c and d: Show the surgical cavity after white light resection (WLR). The bone fluoresces in the green used here as an overlay to provide image orientation.

Histopathology and Volume Calculations

Typical H&E stained sections are illustrated in Figures 4 to 8. The morphology of the VX2 tumor is seen in Figure 4, showing the invasive characteristics, with the proliferating tumor margin showing protrusions, and distant tumor nests extending in the normal brain. Figure 5 shows a section of WLR tissue, which is mostly characterized by a high density of tumor cells and a region of normal brain adjacent to tumor. Figure 6 illustrates a section of FGR tissue, with a small area of infiltrative tumor cells and a larger area of brain adjacent to tumor. In two of the 14 animals, where FGR was incomplete, relatively large volumes of residual tumor were present. In seven other animals, only small volumes of residual tumor were found inside the surgical cavity (Fig. 7). In the remaining, five animals no residual tumor could be found post-FGR. In several animals, sections of the whole brain post-FGR revealed tumor cells more than 0.5 mm away from the surgical cavity and, therefore, beyond the detection depth of this device [12] (Fig. 8); in some cases tumor invaded the ventricles and choroid plexus and extended to the opposite hemisphere.

Volumes of resected tumor tissue and resected brain adjacent to tumor were calculated and the averages and

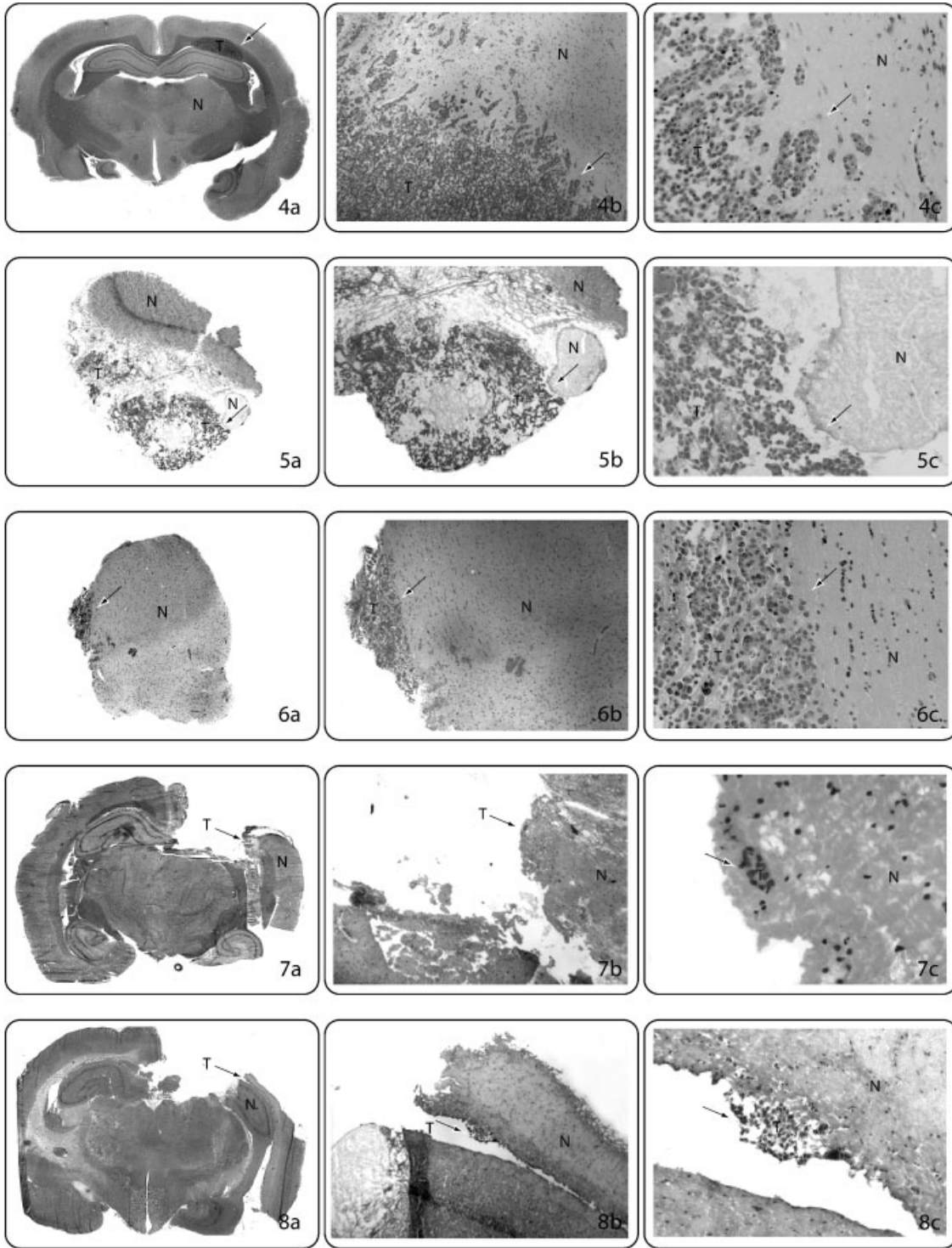
range of values are listed in Table 1. The tumor-to-normal ratio of white light resected tissues was calculated for each animal, and gave a mean of $47 \pm 31\%$, i.e., almost half of the resected tissue was tumor. The corresponding value for FGR tissue was $12 \pm 15\%$. The percentage of tumor resection completeness and RT were then calculated and are listed in Table 2 and a scatter plot of the residual tumor is shown in Figure 9. Using FGR in addition to WLR significantly increased completeness of tumor resection by an average factor 1.4, from 68 ± 38 to $98 \pm 3.5\%$ ($P=0.010$), while the residual tumor in the whole brain decreased by an average factor of 16-fold from 32 ± 38 to $2.0 \pm 3.5\%$ of the total tumor volume ($P=0.010$). These values include three animals where the tumor was not visible using white light but had a small region of fluorescence. It could be argued that this situation will not occur in patients, and that these animals should be excluded. Doing so, gave an increase in completeness of tumor resection by a factor of 1.1 from 86 ± 12 to $98 \pm 3.8\%$ ($P=0.008$), and a decrease in residual tumor in whole brain by an average factor 7, from $14 \pm 12\%$ to $2.0 \pm 3.8\%$ ($P=0.008$). However, including these three animals also supports the hypothesis that more tumor can be resected under fluorescence guidance compared with white light visualization alone.

DISCUSSION

Increased Brain Tumor Resection

The above results show that fluorescence image-guided resection using ALA-induced PpIX enables identification and resection of significantly more tumor than can be

achieved by white-light resection alone. The high degree of tumor resection completeness achieved with WLR+FGR ($98 \pm 3.5\%$) is close to the value of $>98\%$ that has been associated clinically with improved survival [7]. The very large variance in tumor resection completeness by white light, as evidenced by the standard deviation around the



(Figs. 4 to 8).

TABLE 1. Mean \pm Standard Deviation and Range of Resected Tissue Volumes, the Fraction of Tumor, and the Tumor-to-Normal Ratio for WLR and FGR Tissues, Based on H&E Stained Serial Sections

	White light resected tissues			Fluorescence resected tissues			Whole brain
	Resected volume (mm ³)	T _w tumor volume (mm ³)	T/N ratio (%)	Resected volume (mm ³)	T _f tumor volume (mm ³)	T/N ratio (%)	T _{wb} residual tumor volume (mm ³)
Mean	72 \pm 59	48 \pm 45	47 \pm 31	105 \pm 101	8 \pm 12	12 \pm 15	2.2 \pm 6.4
Range	0–176	0–162	0–92	6–395	1–42	1–14	0–24

FGR, fluorescence guided resection; WLR, white light resection; H&E, hematoxylin and eosin; RT, residual tumor.

mean (68 \pm 38%), is markedly reduced using additional fluorescence guidance (98 \pm 3.5%), even although there was a large range of initial tumor sizes and residual tumor after WLR. This suggests that fluorescence guidance not only increases completeness of resection, but also enables more consistent resections between cases.

Resection of Normal Brain

This study differs from other published reports of FGR, in that we saved all resected tissues for histology to determine whether normal brain tissue is also removed during FGR. We found a significant amount of normal brain adjacent to tumor was also resected. There are two main potential explanations for this. The first is that there is detectable ALA-PpIX fluorescence in normal tissue. This is unlikely, based on previous studies that have shown very low ALA-PpIX levels in normal brain tissues with intact BBB [17–20,25], even at high ALA administered doses. A more likely cause is a scaling artifact as a result of the resection technique, where a micro pituitary forceps with a 2-mm tip was used to resect tissues. This is fairly large relative to the tumor size and the rabbit brain, and may have resulted in over resection. This should be much less of a problem in patients, where the resection instruments are relatively small compared to the tumor size. Clinically, more accurate resection techniques could also be used, such as gentle suction and ultrasonic aspiration, which could not be used here because all resected tissues had to be saved for histology. Nevertheless, resecting normal brain tissue adjacent to tumor may be hard to avoid completely due to tumor infiltration.

Fluorescence Quantification

Based on this study, translating FGR to the clinic will require further investigation into the extent of PpIX fluorescence in normal brain tissue (both in absolute terms and relative to tissue autofluorescence at the excitation and emission wavelengths) and, hence, the extent of normal tissue removal (false positives). It will be critical to quantify the fluorescence signal in order to minimize (1) subjective fluorescence image interpretation, which could result in inter-observer variations, and (2) artifacts due to variations in tissue optical properties (e.g., local blood absorption) that may not be related to malignancy [29]. In the present study, the full quantitative capabilities of the imaging system could not be exploited, as explained above, so that we obtained relatively poor anatomical definition and the fluorescence signal was only partially quantitative. This is less of a problem in clinical use because of the larger resection cavity and more complete hemostasis [12].

Limitations of the FGR Technique

In the majority of animals complete tumor resection was not achieved due to small tumor cell nests (2 \pm 3.5% of the total tumor volume) in the surgical cavity that were undetectable by fluorescence. These could be considered as false negatives for this particular device, ALA dose and administration time. Also, in some cases where tumor invaded beyond the surgical cavity, this would not be detectable by fluorescence imaging of the cavity, since the effective tissue sampling depth of the blue-light excitation below the exposed tissue surface is less than 0.5 mm [12].

Fig. 4. Coronal section showing VX2 tumor (T) in the left hemisphere proliferating into the normal (N) brain, and distant tumor cell nests. The arrow indicates the same point in each image using (a) 1 \times , (b) 2.5 \times , and (c) 20 \times objectives. The same convention is used also in Figures 5 to 8.

Fig. 5. Section of WLR tissue with areas of tumor and normal tissue.

Fig. 6. Section of FGR tissue with a small area of tumor and a larger area of normal brain.

Fig. 7. Coronal section of the brain showing the resection cavity in the left hemisphere after WLR and additional FGR. Here, small amounts of residual tumor were found at the surface of the resection cavity. These can be considered false negative for fluorescence detection.

Fig. 8. Coronal section of the brain showing the resection cavity in the left hemisphere after WLR and additional FGR. Here, small amounts of residual tumor were found beyond the surface of the resection cavity, and were not be detectable by fluorescence imaging.

TABLE 2. Mean \pm Standard Deviation and Range of Tumor Resection Completeness (TRC) and RT for Respectively WLR, Fluorescence Resection and the Combination

	Tumor resection completeness (%)			RT (%)		
	TRC _w	TRC _f	TRC _{w+f}	RT _w	RT _f	RT _{w+f}
Mean	67.9 \pm 38.4	30.1 \pm 38.1	98.0 \pm 3.5	32.1 \pm 38.4	69.9 \pm 38.1	2.0 \pm 3.5
Range	0.0–97.8	1.8–99.3	88.6–100.0	2.2–100.0	0.0–98.2	0.0–11.4

TRC, tumor resection completeness.

This suggests that (1) more sensitive fluorescence detection could be advantageous, and (2) an adjuvant therapy applied post-resection that is capable of targeting small tumor nests and invasive tumor, such as photodynamic therapy, may be of further benefit, which is the focus of ongoing studies [30,31].

Limitations of the Present Preclinical Study

Similar to the ALA doses and time interval used in clinical work by Stummer et al. [8,23], this preclinical study was performed at fixed ALA dose (20 mg/kg) and fixed time interval (4 hours) between ALA administration and surgery, which are not necessarily optimal. These parameters will likely affect the sensitivity and specificity of the fluorescence detection in tumor tissue. High sensitivity is

required in order to minimize the residual tumor post-resection, while high specificity will allow the surgeon to avoid removing excessive amounts of normal brain tissue. However, the latter may be less critical, since clinical judgment will always prevail in determining if tissue, whether fluorescent or not, can be removed safely.

Residual tumor was determined accurately in this study since the whole brain was removed, cut in serial sections and examined by histology. Clinically, post-operative MR images are normally used to determine residual tumor. Hence, it will be important to investigate the relationship between the fluorescence signal and MR contrast of residual tumor. We will address these issues in future clinical trials by optimizing the ALA dose and administration time and investigating the correlation between the fluorescence signal and MR contrast in glioma patients.

Future Technology Development

In an effort to address the above limitations, several technological improvements are being considered as part of our ongoing work. More sensitive CCD detectors with higher dynamic range have recently become available that use on-the-chip amplification. Multiple detectors could allow simultaneous acquisition of multiple spectral windows, avoiding the long acquisition times as is the case with our current filter wheel and a single detector. The excitation irradiance used in this study was low (6 mW cm⁻²). With existing Xenon arc lamps and improved optics this can be increased by a factor 10 or more. Another option to increase excitation irradiance is using raster scanning with a relatively high power pencil beam [32]. Depth resolution could be improved by utilizing longer excitation wavelengths and raster scanning, considering both single- and multi-photon excitation [33], which could also allow depth tomography. The fluorescence signal may be further increased by utilizing fluorophores and/or nanocrystals selected for high fluorescence yield, which might then be labeled to antibodies for tumor selective targeting [34,35]. In terms of quantitation, it would be advantageous to obtain fluorescence signal that depends only on the local fluorophore concentration. Several spectroscopic methods suggested in the literature have been evaluated by Sterenberg et al. [29] using multiple excitation and/or detection wavelengths, which could also be utilized for imaging. Currently, we are developing fluorescence imaging systems considering the above.

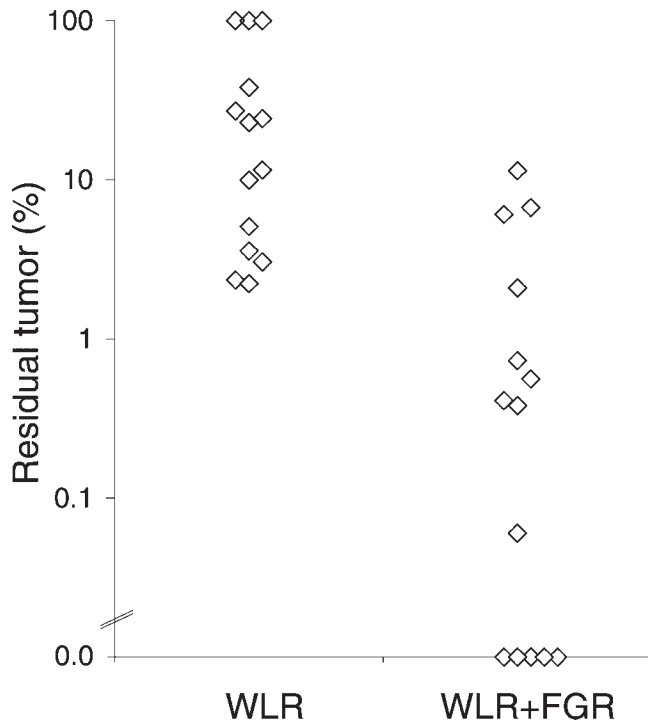


Fig. 9. Scatter plot of the percentage of residual tumor using WLR only versus WLR + FGR. In five animals, no residual tumor was found histologically after WLR + FGR.

ACKNOWLEDGMENTS

Instrument development was supported by Photonics Research Ontario. Statistical advice of Dr. Judith Abrahams is gratefully acknowledged. DUSA Pharmaceuticals NY kindly provided the ALA and Brian C. Wilson received this support. Microscopes, image processing software, and support were available through the Advanced Optical Microscope Facility (AOMF) at the Ontario Cancer Institute, supported by the Canadian Foundation for Innovation.

REFERENCES

- Shapiro WR, Green SB, Burger PC, Mahaley MS, Jr., Selker RG, VanGilder JC, Robertson JT, Ransohoff J, Mealey J, Jr., Strike TA, et al. Randomized trial of three chemotherapy regimens and two radiotherapy regimens and two radiotherapy regimens in postoperative treatment of malignant glioma. Brain Tumor Cooperative Group Trial 8001. *J Neurosurg* 1989;71(1):1–9.
- Walker MD, Green SB, Byar DP, Alexander E, Jr., Batzdorf U, Brooks WH, Hunt WE, MacCarty CS, Mahaley MS, Jr., Mealey J, Jr., Owens G, Ransohoff J II, Robertson JT, Shapiro WR, Smith KR, Jr., Wilson CB, Strike TA. Randomized comparisons of radiotherapy and nitrosoureas for the treatment of malignant glioma after surgery. *N Engl J Med* 1980;303(23):1323–1329.
- Rostomily RC, Spence AM, Duong D, McCormick K, Bland M, Berger MS. Multimodality management of recurrent adult malignant gliomas: Results of a phase II multiagent chemotherapy study and analysis of cytoreductive surgery. *Neurosurgery* 1994;35(3):378–388; discussion 388.
- Nitta T, Sato K. Prognostic implications of the extent of surgical resection in patients with intracranial malignant gliomas. *Cancer* 1995;75(11):2727–2731.
- Devaux BC, O'Fallon JR, Kelly PJ. Resection, biopsy, and survival in malignant glial neoplasms. A retrospective study of clinical parameters, therapy, and outcome. *J Neurosurg* 1993;78(5):767–775.
- Yoshida J, Kajita Y, Wakabayashi T, Sugita K. Long-term follow-up results of 175 patients with malignant glioma: Importance of radical tumour resection and postoperative adjuvant therapy with interferon, ACNU and radiation. *Acta Neurochir* 1994;127(1–2):55–59.
- Lacroix M, Abi-Said D, Fournier DR, Gokaslan ZL, Shi W, DeMonte F, Lang FF, McCutcheon IE, Hassenbush SJ, Holland E, Hess K, Michael C, Miller D, Saway R. Multivariate analysis of 416 patients with glioblastoma multiforme: Prognosis, extent of resection, and survival. *J Neurosurg* 2001;95(2):190–198.
- Stummer W, Stepp H, Moller G, Ehrhardt A, Leonhard M, Reulen HJ. Technical principles for protoporphyrin-IX-fluorescence guided microsurgical resection of malignant glioma tissue. *Acta Neurochir* 1998;140(10):995–1000.
- Murray KJ. Improved surgical resection of human brain tumors: Part I. A preliminary study. *Surg Neurol* 1982;17(5):316–319.
- Kremer P, Wunder A, Sinn H, Haase T, Rheinwald M, Zillmann U, Albert FK, Kunze S. Laser-induced fluorescence detection of malignant gliomas using fluorescein-labeled serum albumin: Experimental and preliminary clinical results. *Neurolog Res* 2000;22(5):481–489.
- Poon WS, Schomacker KT, Deutsch TF, Martuza RL. Laser-induced fluorescence: Experimental intraoperative delineation of tumor resection margins. *J Neurosurg* 1992;76(4):679–686.
- Yang VX, Muller PJ, Herman P, Wilson BC. A multispectral fluorescence imaging system: Design and initial clinical tests in intra-operative Photofrin-photodynamic therapy of brain tumors. *Lasers Surg Med* 2003;32(3):224–232.
- Shinoda J, Yano H, Yoshimura S, Okumura A, Kaku Y, Iwama T, Sakai N. Fluorescence-guided resection of glioblastoma multiforme by using high-dose fluorescein sodium. Technical note. *J Neurosurg* 2003;99(3):597–603.
- Hebeda KM, Saarnak AE, Olivo M, Sterenborg HJ, Wolbers JG. 5-Aminolevulinic acid induced endogenous porphyrin fluorescence in 9L and C6 brain tumours and in the normal rat brain. *Acta Neurochir* 1998;140(5):503–512.
- Kelty CJ, Brown NJ, Reed MWR, Ackroyd R. The use of 5-aminolaevulinic acid as a photosensitizer in photodynamic therapy and photodiagnosis. *Photochem Photobiol Sci* 2002;3:149–224.
- Stummer W, Gotz C, Hassan A, Heimann A, Kempfski O. Kinetics of Photofrin II in perifocal brain edema. *Neurosurg* 1993;33(6):1075–1081; discussion 1072–1081.
- Olivo M, Wilson BC. Mapping ALA-induced PPIX fluorescence in normal brain and brain tumour using confocal fluorescence microscopy. *Int J Oncol* 2004;25(1):37–45.
- Lilge L, Olivo MC, Schatz SW, MaGuire JA, Patterson MS, Wilson BC. The sensitivity of normal brain and intracranially implanted VX2 tumour to interstitial photodynamic therapy. *Br J Cancer* 1996;73(3):332–343.
- Lilge L, Portnoy M, Wilson BC. Apoptosis induced in vivo by photodynamic therapy in normal brain and intracranial tumour tissue. *Br J Cancer* 2000;83(8):1110–1117.
- Lilge L, Wilson BC. Photodynamic therapy of intracranial tissues: A preclinical comparative study of four different photosensitizers. *J Clin Laser Med Surg* 1998;16(2):81–91.
- Olzowy B, Hundt CS, Stocker S, Bise K, Reulen HJ, Stummer W. Photoradiation therapy of experimental malignant glioma with 5-aminolevulinic acid. *J Neurosurg* 2002;97(4):970–976.
- Stummer W, Ennis SR, Betz AL, Keep RF. In vitro and in vivo porphyrin accumulation by C6 glioma cells after exposure to 5-aminolevulinic acid. *Cerebral Blood Flow Metab* 1999;19(1):79–86.
- Stummer W, Novotny A, Med CN, Stepp H, Goetz C, Bise K, Reulen HJ. Fluorescence-guided resection of glioblastoma multiforme by using 5-aminolevulinic acid-induced porphyrins: A prospective study in 52 consecutive patients. *J Neurosurg* 2000;93(6):1003–1013.
- Moan J, Ma LW, Juzeniene A, Iani V, Juzenas P, Apricena F, Peng Q. Pharmacology of protoporphyrin IX in nude mice after application of ALA and ALA esters. *Int J Cancer* 2003;103(1):132–135.
- Wu SM, Ren QG, Zhou MO, Peng Q, Chen JY. Protoporphyrin IX production and its photodynamic effects on glioma cells, neuroblastoma cells, and normal cerebellar granule cells in vitro with 5-aminolevulinic acid and its hexylester. *Cancer Lett* 2003;200(2):123–131.
- Ennis SR, Novotny A, Xiang J, Shakui P, Masada T, Stummer W, Smith DE, Keep RF. Transport of 5-aminolevulinic acid between blood and brain. *Brain Res* 2003;959(2):226–234.
- Peng Q, Warloe T, Berg K, Moan J, Kongshaug M, Giercksky KE, Nesland JM. 5-Aminolevulinic acid-based photodynamic therapy. Clinical research and future challenges. *Cancer* 1997;79(12):2282–2308.
- Peng Q, Berg K, Moan J, Kongshaug M, Nesland JM. 5-Aminolevulinic acid-based photodynamic therapy: Principles and experimental research. *Photochem Photobiol* 1996;65(2):235–251.
- Sterenborg HJ, Saarnak AE, Frank R, Motamedi M. Evaluation of spectral correction techniques for fluorescence measurements on pigmented lesions in vivo. *J Photochem Photobiol B* 1996;35(3):159–165.
- Bisland SL, Lilge LD, Lin A, Wilson BC. Metronomic photodynamic therapy (mPDT) for intracranial neoplasm: Physiological, biological, and dosimetry considerations. *Proc SPIE* 2003;5142:9–17.
- Wilson BC, Bisland SK, Bogaards A, Lin A, Moriyama EH, Zhang K, Lilge LD. Metronomic photodynamic therapy (mPDT): Concepts and technical feasibility in brain tumor. *Proc SPIE* 2003;4952:23–31.

32. Pogue BW, Gibbs SL, Chen B, Savellano M. Fluorescence imaging in vivo: Raster scanned point-source imaging provides more accurate quantification than broad beam geometries. *Technol Cancer Res Treat* 2004;3(1):15–21.
33. Zipfel WR, Williams RM, Webb WW. Nonlinear magic: Multiphoton microscopy in the biosciences. *Nat Biotechnol* 2003;21(11):1369–1377.
34. Akerman ME, Chan WC, Laakkonen P, Bhatia SN, Ruoslahti E. Nanocrystal targeting in vivo. *Proc Natl Acad Sci USA* 2002;99(20):12617–12621.
35. Chan WC, Maxwell DJ, Gao X, Bailey RE, Han M, Nie S. Luminescent quantum dots for multiplexed biological detection and imaging. *Curr Opin Biotechnol* 2002;13(1):40–46.